

Programmable Soft Robotics Based on Nano-Textured Thermo-Responsive Actuators

Dong Jin Kang^{a, b§}, Seongpil An^{a§}, Alexander L. Yarin^{a*} and Sushant Anand^{a*}

Soft robotic systems are increasingly emerging as robust alternatives to conventional robotics. Here we demonstrate the development of programmable soft actuators based on volume expansion/retraction accompanying liquid-vapor phase transition of a phase-change material confined within an elastomer matrix. The combination of a soft matrix (a silicone-based elastomer) and the embedded ethanol-impregnated polyacrylonitrile nanofiber (PAN NF) mat makes it possible to form a sealed compound device that can be operated by changing the actuator temperature above/below than the boiling point of ethanol. The thermo-responsive actuators based on this principle demonstrate excellent bending ability at a sufficiently high temperature ($> 90\text{ }^{\circ}\text{C}$) - comparable with compressed air based soft actuators. The actuator mechanism presented herein is easy to manufacture, easy to automate and recyclable. Finally, the actuation mechanism can be incorporated in wide variety of shapes and configurations making it possible to obtain tunable and programmable soft robots that could find application in wide variety of industrial applications.

Introduction

Traditional robotic systems are built using stiff materials with actuation occurring via connecting joints. While such systems are typically rugged, can operate in harsh environments and lift significant loads, they can also be costly and require significant energy inputs. There is a growing interest in recent years to overcome such constraints by building soft robots based on 'soft materials'. Soft robots can provide fine motion even using simple force controls while also being cost-effective, lightweight, and flexible compared to traditional rigid robotic systems.¹⁻⁷ Furthermore, components constituting robots such as grippers in actuators made of soft materials can be easily programmed for diverse applications, thus paving way for large degree of autonomy in soft robots.⁸⁻¹⁰ There are two essential constituents for building soft robots; the nature of soft material chosen as a body, and the nature of mechanism used to actuate such soft material. To design high performance soft robotics, a wide variety of soft materials have been

explored, such as responsive polymers,^{11, 12} hydrogels,^{13, 14} ionic exchange materials,¹⁵ elastomers,¹⁶⁻¹⁹ and electro-active polymers.^{20, 21} Soft actuators made of above-mentioned materials have been activated by means of electromechanical methods such as pressurized fluids,²² compressed air,^{23, 24} electricity,^{25, 26} magnetic forces^{27, 28} and thermal energy.²⁹ Such actuation methods although very successful, can also be prohibitively energy consuming¹⁶ and often require additional equipment or wet environments^{11, 12, 30} that can limit their applications.^{15, 17, 23, 24} Recently, an actuating mechanism based on thermal expansion/contraction of wax-based phase change materials (PCMs) from liquid-to-solid state has emerged as a promising alternative to the above-mentioned conventional electrochemical actuation methods. Such method can be used with a broad range of soft materials and is conceptually simpler to operate.³¹⁻³⁶ However, there are two key challenges related to applicability of such actuators for general robotics-related applications. Firstly, such actuators relied on liquid-solid phase transition during which the volume change of paraffin wax is less than 15% that limits their performance. Secondly, the hardness of solid paraffin is incompatible with soft robotics. To overcome such challenges, PCM actuators relying on liquid-vapor phase transition have been proposed. Fast, agile, and reversible soft robots based on PCM have been obtained using liquids with high vapor pressure³⁷ and aqueous solvents.³⁸ In a recent work for example, volume-changing

^a Department of Mechanical and Industrial Engineering, University of Illinois at Chicago, 842 W. Taylor St., Chicago, Illinois 60607-7022, USA.

^b Current Address: INM-Leibniz Institute for New Materials, Saarbrücken, Germany
E-mail: ayarin@uic.edu, sushant@uic.edu
Electronic Supplementary Information (ESI) available: [details of any supplementary information available should be included here]. See 10.1039/c8nr08215d

§These authors contributed equally to this work.

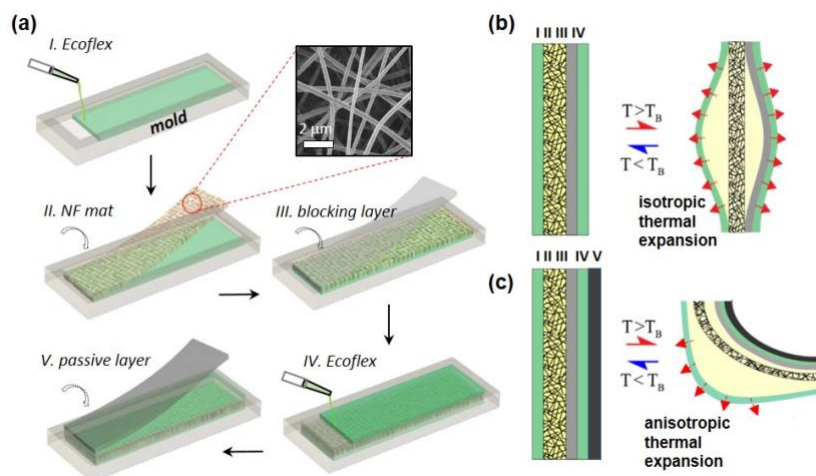


Fig. 1 Schematic illustration of two different types of structures and their actuation based on liquid-vapor phase change in a thermo-responsive soft actuator. (a) Preparation procedures of multi-layered soft actuator. (b) Structure of stationary soft actuator, with the four layers including an elastomeric matrix, polymer nanofiber (NF) mat imbided with ethanol, and a blocking layer. (c) A single bending structure of such soft actuator, with the five layers including an elastomeric matrix, polymer NF mat imbided with ethanol, blocking layer, and a stiffer passive layer. The scale bar is 2 μm .

soft actuators based on liquid-vapor phase transition of ethanol were shown to reveal excellent performance.³⁹ The operation of such device was based on micro-bubble formation of the ethanol trapped in elastomer. However, such approach is limited by the lack of control over the bubble sizes, which can eventually impose constraints on the system, such as limiting the extent for actuation.

Here, we develop a novel programmable thermo-responsive soft actuator based on liquid-vapor phase change that overcomes many of the above-mentioned limitations. The high performance thermo-pneumatic soft actuator is comprised of multi-layered structures consisting of the ethanol-infused nanofiber (NF) mat encased in a biocompatible elastomer. In this design, ethanol serves as a PCM capable of triggering the reversible soft actuator near its boiling point (T_B). The use of ethanol as a PCM allows the actuator to develop strains up to 200% near its boiling point that can be harnessed to cause bending motion with bending angle approaching 180°. The use of NF mats provides a natural means for a uniform distribution of ethanol due to capillary imbibition within the entire elastomer matrix resulting in smoothly occurring volume and shape changes of the elastomer matrix.⁴⁰ The proposed actuator system is such that it can operate without additional electric power or pressure-regulating equipment, thus making it possible to design simply programmable and applicable soft robotics without complex processes. Furthermore, as will be shown later, the thermo-pneumatic actuating mechanism can be easily incorporated into diverse forms, such as artificial grippers or walking robots.

Experimental section

Materials Polyacrylonitrile (PAN, $M_w = 150$ kDa) and *N,N*-dimethylformamide (DMF, 99.9%) were obtained from Sigma-Aldrich (USA). Ethanol, 200 proof, anhydrous, $\geq 99.5\%$ was purchased from Sigma-Aldrich. Fluorescein sodium salt was obtained from Sigma-Aldrich and it was mixed with ethanol for visualization purposes. Commercial Ecoflex 00-30 and 00-35 were obtained from Smooth-On (USA) (Young's modulus and Poisson's ratio are 29.5 kPa and 0.4999, respectively⁴¹). An aluminum mold was designed for shaping soft actuators. A paper towel for a passive mat was purchased from the local market, (thickness: 150 ~ 200 μm , Kleenex Drycell, USA).

Electrospinning setup An 8 wt% PAN solution in DMF was electrospun onto a rotating drum with a flow rate of 0.3 mL/h and a high DC voltage of 7.5 kV using an 18-gauge needle (Sigma-Aldrich, USA), a syringe pump (New Era Pump System, USA), and a DC voltage supply (Glassman High Voltage, USA), which facilitated the production of a large-area non-woven nanofiber (NF) mat.⁴² The distance between the needle and the drum collector in the electrospinning setup was 10 cm. The NF mat formed on the drum was detached and then cut into rectangular 1 \times 10 cm² pieces.

Characterization The morphology and thickness of PAN NF mat were examined by a field emission scanning electron microscope (FE-SEM, JSM-6320F, JEOL, USA). The fiber diameter, size distribution and the radius of curvature were analysed by Image J image analysis software. Strain-induced stress was characterized by Digital Force Gauge (Mark-10 series 5, $\pm 0.1\%$ accuracy) to measure the pull force of bending soft actuator. The operation temperature was controlled by SHEL LAB vacuum oven (SVAC-1) without vacuum control. The images and movies were obtained using digital cameras D3200 and D5500 (Nikon, Japan).

Results and discussion

Our thermo-pneumatic actuator is comprised of a five-layered structure. **Fig. 1a** shows the procedure used to fabricate such a structure. At the first step, a rectangular aluminum mold was designed in which an elastomer (Ecoflex 00-30) is poured and partially cured for 4 min. Ecoflex 00-30 elastomer was chosen in this work because it has a low Young's modulus and can undergo up to 800% change in strain without permanent damage.⁴¹ The partial cure was necessary to prevent wicking of liquid Ecoflex in the NF mat. At the second step, a NF mat made of oleophilic polyacrylonitrile (PAN) with the average fiber diameter of 292 ± 42 nm and the inter-fiber pore size of $0.306 \pm 0.157 \mu\text{m}^2$ (see **Fig. S1**) was then gently placed on the partially cured elastomer layer. PAN was chosen in our work because PAN NF mats have been shown to possess highly interconnected pores with a large surface area, making it possible to imbibe large liquid volumes within them.⁴³⁻⁴⁶ It should be emphasized that the presence of PAN NF mat, which is capable of absorbing liquid and spreading it out, is a key point to properly operate our thermal responsive actuator. For example, it is hard to inject ethanol into the resulting Ecoflex actuator deeply without the NF mat because of the absence of imbibition effect by the NF mat. Even though the ethanol is injected into the actuator, a non-uniformly distributed ethanol in the actuator caused the uneven volume expansion of the actuator. At the third step, a paper with high stiffness was used as a blocking layer in order to prevent permeation of Ecoflex liquid that was to be added at the next stage. At the fourth step, Ecoflex 00-30 elastomer was added again on the prior-assembled matrix followed by placement of the rigid paper to act as a passive layer at the fifth step. As will be discussed later, this fifth layer plays a very important role in enabling actuation in our design. After the entire structure has been assembled, it was kept at 60 °C for 7 min to cure the elastomers completely. The mold structure allowed the elastomer to spread at the edges that then became automatically sealed during the curing process. The procedure described above can be completed in matter of minutes making it possible to fabricate large number of soft actuators quickly. Finally, 0.95 g of ethanol mixed with green dye was injected into the soft actuator through a 25-gauge needle-equipped syringe, and the injection tunnel was then sealed using Ecoflex 00-35 that has $\sim 50\times$ curing rate compared to that of Ecoflex 00-30. The green dye was added to allow visualization of liquid-vapor phase change transition

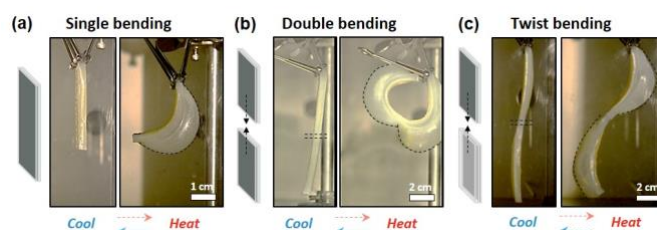


Fig. 2 Different possible designs of thermo-responsive bending soft actuators. (a) Single bending structure and its shapes activated at a switch from 25 °C to 90 °C. (b) Double bending structure, which combined two single bending actuators in the same bending direction, and its shapes activated at a switch from 25 °C to 90 °C. The radius of curvature in this configuration was measured as 9.4 mm (c) Twist bending structure, which combined two single bending actuators with the opposite bending directions, and its shapes activated at a switch from 25 °C to 90 °C.

as they occurred within the elastomer matrix (see **Fig. S2**). Once assembled, the composite structure temperature (T_0) was brought sufficiently close to the boiling temperature of ethanol (T_B) so that liquid-vapor transition and the accompanying vapor expansion can provide sufficient force to trigger volume/shape change. The reversible actuation is achieved by turning heat on/off in order to control phase transitions from liquid to vapor and vice versa.

As indicated earlier, the passive layer plays an important role in the actuator of our design. In the absence of the passive layer, we obtain a nearly symmetric structure of soft actuator with identical elastomer layers on either side of the NF mat. As thermal energy is supplied to this structure, the liquid-vapor transition leads to isotropic vapor expansion (**Figs. 1b** and **S3**). Such isotropic expansion can possibly be used to lift objects or for pumping liquids, however, this configuration is limited in its applications especially for actuation along a unique direction. On the other hand, addition of the fifth passive layer with higher stiffness facilitates asymmetry in the composite structure because of which a unidirectional bending motion occurs when this composite structure is heated (**Fig. 1c**). Such configuration is the key to obtain enhanced programmable motions (expansion or bending) of the soft actuator and hence can find wide-ranging applications.

An example of the unidirectional bending motion achieved by the configuration elaborated in **Fig. 1c** is shown in **Fig. 2a**. In this configuration, the 1st Ecoflex layer swells up to 170% at $T_0 > T_B$ compared to the initial direction (note that the bending of soft actuator was similarly characterized by curvature in ref. 41). As a consequence, the actuator exhibits a large bending angle (up to 180°) and radius of curvature (~ 17.5 mm). The concept of our thermo-pneumatic actuator is highly versatile and apart from the single

unidirectional bending actuator illustrated above, several other configurations with additional degrees of freedom can also be achieved through appropriate modifications. As an example, by attaching two single bending actuators at their ends with the composite layers aligned in same direction results in formation of a double bending actuator (**Fig. 2b**). Such structure as will be illustrated later can be used as a gripper for holding and lifting objects. In another example, we could also achieve a twisting type actuator by attaching two single bending actuators at their ends with the composite layers aligned in opposite direction to each other (**Fig. 2c**). Such twisting motion is impossible to be achieved by human beings and can potentially be applied for obtaining complex motions. As we will demonstrate next, the designs discussed above can be applied as an artificial finger, worms in soft robots, thermally responsive flowers, *etc.*

Having identified the methods to produce actuators that could lead to different type of actuating configurations, we next sought to study the factors affecting the performance of our thermo-responsive actuators. The performance of an actuator may depend upon several factors, e.g. operational conditions (i.e. applied thermal energy), and the number of passive layers. Thus, at the next step, we performed extensive tests to understand the performance of a unidirectional single actuator (e.g. the one shown in **Fig. 2a**) as a function of above-mentioned factors. We measured the average tip speed of actuation (v) of a single bending actuator and maximum possible curvature as a function of temperature from 60 °C to 140 °C (**Figure 3a** and Supporting **Movie S1**). The average velocity was found using the relation $v = \Delta l / t$, where Δl is the change in the position of the actuator tip from the initial stage to the final stage, and t is the time when the actuator reached the maximum bending angle. The snapshot of images of actuator taken during its operation at its highest bending position (**Fig. 3a**) clearly show that increasing temperature leads to higher bending. We find that the actuator shows negligible bending until heated to the boiling point of ethanol. Only a small bending deformation is observed at 80 °C, even though this temperature is above T_B of ethanol. This is because further evaporation is suppressed by inevitable pressure growth, which happens once the ethanol vapor is trapped in a confined space. As shown in **Fig. 3b**, both the speed and the radius of curvature (K_{radius}) are dramatically changed from $15.3 \mu\text{m}\cdot\text{s}^{-1}$ to $281.3 \mu\text{m}\cdot\text{s}^{-1}$ and 69.5 mm to 19.5 mm, respectively as the temperature changes from 80 °C to 100 °C, respectively. The speed increases up to $1325.8 \mu\text{m}\cdot\text{s}^{-1}$ and

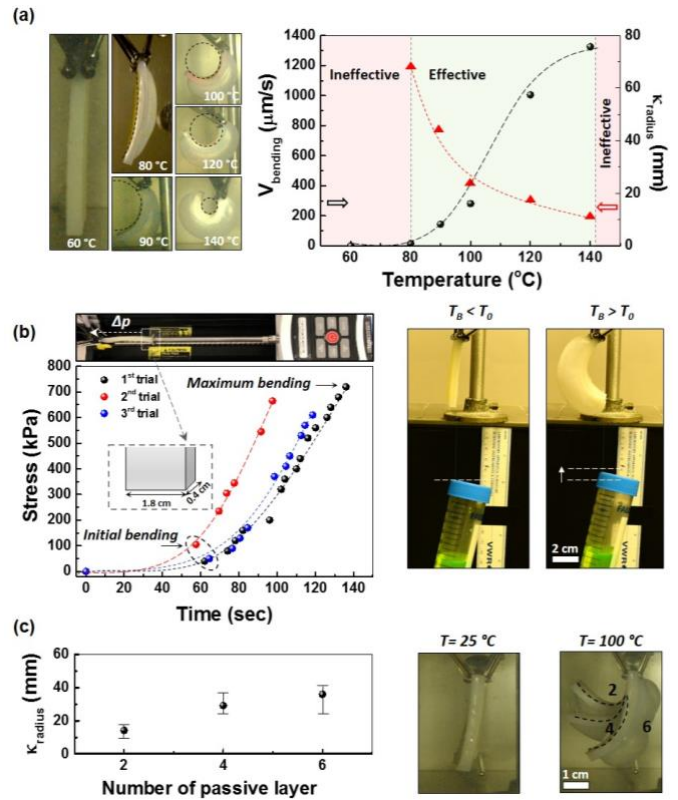


Fig. 3 The effective operational conditions and the effect of the number of passive layers. (a) The velocity of actuation of a single bending actuator and its radius of curvature at the maximum bending angle as a function of temperature from 60 °C to 140 °C. (b) Measurement of the stress induced by structural deformation of a single bending actuator as function of time at 100 °C. On the right, a single bending actuator lifts the weight of 40 g at $T_0 > T_B$ (78.4 °C). (c) The optimization of the bending efficiency of single bending actuators as a function of the number of passive layers (from 2 to 6 layers) at 100 °C.

the radius of curvature decreases to 11.3 mm at 140 °C. Operating the actuator beyond temperature of 140 °C leads to loss of elasticity (**Fig. S4**) even though it still demonstrates an excellent actuation performance (i.e. we still achieve high bending angles or high tip velocities). These results demonstrate that the increase in vapor pressure by increasing temperature results in decrease of the maximum curvature of a single bending actuator⁴⁷ and the effective operational temperature for actuator using ethanol is between 90 °C and 140 °C. Next we sought to determine the structural deformation-induced stress generated by a single bending actuator (with the contact area of 0.72 cm²) as a function of time at ~100 °C. One end of the single bending actuator was attached to a digital force gauge (Mark-10 series 5, $\pm 0.1\%$ accuracy) and the stress was then measured during bending deformation with three trials using different samples (see Characterization in Experimental Section). During the first 60s, no significant stress developed in the system because the thermally

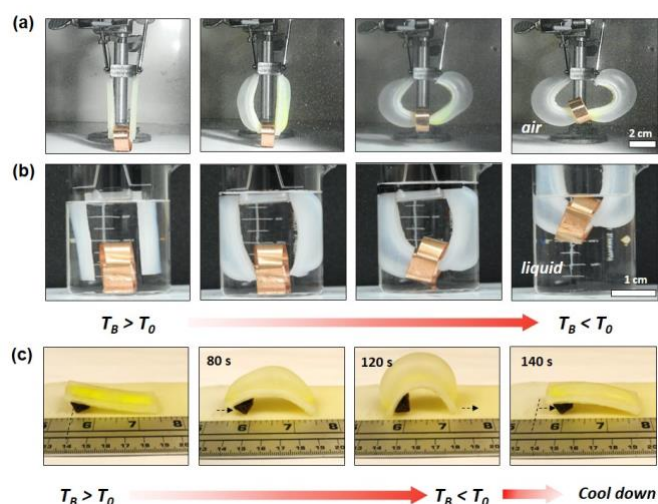


Fig. 4 Bio-inspired soft robotics. (a) Operation of artificial fingers in air using bending thermo-responsive soft actuator at 100 °C. (b) Operation of fingers within a polymeric liquid (100 cSt silicone oil) at 100 °C, (c) Soft robot designed as a larva using single bending soft actuator subjected to varying temperature.

insulative nature of elastomer materials results in a delay in boiling of ethanol. Beyond 60s, we find there is critical stress that develops in beginning of the bending motion (40 kPa, 42 kPa, and 75 kPa; cf. **Fig. 3b**). The stress continuously increases up to 132 s and reached the level of 650 ~ 720 kPa. The maximum stress demonstrated by the present soft actuator is comparable with those revealed by previous soft actuator systems based on compressed air or with the electrically-induced soft actuators.⁴⁸ These measurements clearly suggest that the unidirectional single actuator can develop sufficient stress to lift objects/actuation in short durations. Thus next, we tested a single bending actuator as an artificial muscle by attaching a plastic tube at its end and filling it with different amounts of water. We found that a single actuator was capable of lifting up to 40 g of weight when supplied at a temperature above T_B of ethanol as shown in **Fig. 3b**. This test demonstrates that the present soft actuator can be successfully applied as a robotic arm, and it can lift 40 times the weight of ethanol and PAN NF. Another important performance measure of an actuator is evaluating if any hysteresis develops in the actuator structure as it is constantly inflated/deflated. To gauge this behavior, we investigated the performance of the soft actuator over 10 cycles (**Fig. S5**). The performance is evaluated by tracking its radius of curvature at each cycle when the actuator temperature exceeds the boiling temperature T_B of ethanol, i.e. $T_0 > T_B$. The radius of curvature during first operation was measured at ~14.1 mm and increased slightly during 10 cycles likely as a result of vapor leakage.

To confirm this aspect, we tested the same sample which was used for cycling test in 1 day (i.e. after a one-day storage after a 10-cycle test). The radius of curvature increased to 42 mm. It clearly indicates that permeability of the encasing matrix affects to repeatability of the actuator action.⁴⁹ It should be emphasized that in the case of need, ethanol can be supplied additionally and the actuator can restore its original capability.

Since our thermo-pneumatic actuator is based on the difference in stiffness of materials, we performed experiments to investigate the actuator performance as a function of the number of passive layers (**Fig. 3c**). Different actuators were made with 2 to 6 passive layers stacked together and their performance was measured at 100 °C. The highest bending deformation was observed with two passive layers (the thickness ≈ 0.3 mm). The radius of curvatures of a single bending actuator with different number of passive layers revealed the values of 14.2 ± 2 mm, 29.2 ± 1.5 mm, and 36 ± 3 mm, with the increasing number of passive layers. Thus the number of passive layer affects the asymmetry responsible for bending.

Above results demonstrate that even in its most basic form (single actuator configuration), the thermo-pneumatic actuation mechanism has sufficient power to lift objects. **Fig. 4** shows a programmable thermo-responsive soft robotic palm comprised of two single-bending fingers that can lift an object (cf. Supporting **Movie S2**). Such finger-type configuration can be applied as an industrial or biomedical gripper in diverse applications. During the actuation, the 1st Ecoflex layer was inflated at $T_0 > T_B$. Then, the incommensurate asymmetric elongation of the soft 1st Ecoflex layer and the 5th passive layer caused buckling on the passive layer, resulting in the lifting motion – similar to folding of the human fingers. Note that the actuator described above did not require connections with an external power supply or any bulky additional equipment such as an air compressor. Furthermore, such actuators can also be operated within viscous liquids. As an example, the actuators in finger-configuration successfully lifted objects while operating within 100 cSt silicone oil and water as shown in **Figs 4b**, **S6b**, and Supporting **Movie S3**. These experiments suggest that the thermos-responsive actuators have the potential to be used inside pipelines even in viscous liquids. Such abilities open up new possibilities for their usage such as performing diagnostics on pipe materials, checking leaks or plugging them etc. In addition, we designed soft robots mimicking biological movements, such as those

of larvae, through a combination of a single bending actuator and a solid leg as shown in **Fig. 4c** and Supporting **Movie S4**. To trigger actuation, we used a heat gun (Wagner Digital Heat Gun, HT3500) which can provide sufficiently high temperatures to surpass T_B of ethanol. As a result of heating, expansion of the soft actuator induces bending deformation, at the same time the solid leg of artificial larvae robot is twitched. On the other hand, during cooling, the artificial larvae robot kicks the ground, causing the robot to walk forward as shown in **Fig. 4c**. Due to the expansion of the soft actuator, the centroid of the larvae robot moves from its bending point towards the front side. One can also envision other configurations where the thermos-pneumatic actuation mechanism could be useful. As an example, several single bending actuators can be combined to form a reversible self-actuated thermo-responsive flower (cf. **Fig. S6a** and Supporting **Movie S5**). A closed flower (the initial shape) fabricated of three single bending actuators is heated above T_B of ethanol and opens as a flower at full blossom. This design can be potentially used for the solar cell panels, which can connect to solar light power generator in order to collect enough sun light when the temperature is increased above its switch temperature.

Conclusion

In summary, we proposed biocompatible thermo-responsive nano-textured soft actuators and demonstrated their capabilities as programmable soft robots. The actuators employ thermally-triggered phase transition (evaporation) of ethanol encased in electrospun nanofiber (NF) mat embedded asymmetrically in a flexible matrix. The maximum bending stress and curvature are comparable with those of the previously studied pneumatic and electrically-triggered soft actuators. In addition, the present soft actuator does not require any additional electric power-supplying or pressure-regulating equipment, which widens its applications in soft robotics. For example, if this soft actuator is installed in a device operated in a desert, it can operate, in principle, with another working fluid employing the surrounding temperature change between day and night, for example, in a palm tree-like tent equipped with such an actuator. In the daytime this device can pitch a tent and make the shade, while it can automatically take down the tent in the night time. Such a mechanism can also be useful for water collection in the desert. Another example would be the alarm sensors in a building. In the event of fire, the sensor based on this actuator can ring the alarm bell by reacting to the temperature change.

Conflicts of interest

There are no conflicts to declare.

Acknowledgements

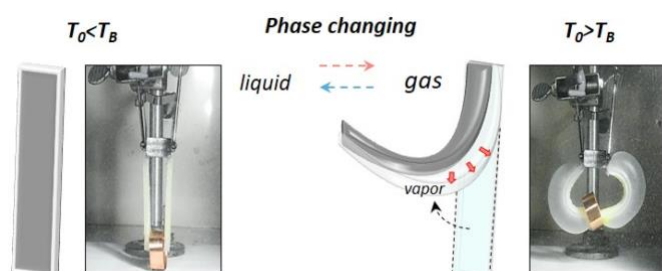
Funding: We thank the support of UIC College of Engineering.

References

- 1 B. Mosadegh, P. Polygerinos, C. Keplinger, S. Wennstedt, R. F. Shepherd, U. Gupta, J. Shim, K. Bertoldi, C. J. Walsh and G. M. Whitesides, *Adv. Funct. Mater.*, 2014, **24**, 2163-2170.
- 2 D. Rus and M. T. Tolley, *Nature*, 2015, **521**, 467-475.
- 3 D. Yang, B. Mosadegh, A. Ainla, B. Lee, F. Khashai, Z. Suo, K. Bertoldi and G. M. Whitesides, *Adv Mater*, 2015, **27**, 6323-6327.
- 4 S. M. Mirvakili and I. W. Hunter, *Adv Mater*, 2018, **30**.
- 5 D. Trivedi, C. D. Rahn, W. M. Kier and I. D. Walker, *Appl. Bionics Biomech.*, 2008, **5**, 99-117.
- 6 C. Majidi, *Soft Robotics*, 2014, **1**, 5-11.
- 7 M. Whitesides George, *Angew. Chem., Int. Ed.*, 2018, **57**, 4258-4273.
- 8 M. Wehner, R. L. Truby, D. J. Fitzgerald, B. Mosadegh, G. M. Whitesides, J. A. Lewis and R. J. Wood, *Nature*, 2016, **536**, 451-455.
- 9 L. Hines, K. Petersen, G. Z. Lum and M. Sitti, *Adv Mater*, 2017, **29**.
- 10 P. Polygerinos, N. Correll, S. A. Morin, B. Mosadegh, C. D. Onal, K. Petersen, M. Cianchetti, M. T. Tolley and R. F. Shepherd, *Adv. Eng. Mater.*, 2017, **19**.
- 11 L. Liu, A. Ghaemi, S. Gekle and S. Agarwal, *Adv Mater*, 2016, **28**, 9792-9796.
- 12 M. Wei, Y. Gao, X. Li and M. J. Serpe, *Polym. Chem.*, 2017, **8**, 127-143.
- 13 Z. Liu and P. Calvert, *Adv Mater*, 2000, **12**, 288-291.
- 14 A. F. Greene, M. K. Danielson, A. O. Delawder, K. P. Liles, X. Li, A. Natraj, A. Wellen and J. C. Barnes, *Chem. Mater.*, 2017, **29**, 9498-9508.
- 15 G. Wu, Y. Hu, Y. Liu, J. Zhao, X. Chen, V. Whoehling, C. Plesse, G. T. M. Nguyen, F. Vidal and W. Chen, *Nat. Commun.*, 2015, **6**.
- 16 R. Pelrine, R. Kornbluh and G. Kofod, *Adv Mater*, 2000, **12**, 1223-1225.
- 17 J. Biggs, K. Danielmeier, J. Hitzbleck, J. Krause, T. Kridl, S. Nowak, E. Orselli, X. Quan, D. Schapeler, W. Sutherland and J. Wagner, *Angew. Chem., Int. Ed.*, 2013, **52**, 9409-9421.
- 18 M. D. Bartlett, N. Kazem, M. J. Powell-Palm, X. Huang, W. Sun, J. A. Malen and C. Majidi, *Proc. Natl. Acad. Sci. U. S. A.*, 2017, **114**, 2143-2148.
- 19 E. J. Markvicka, M. D. Bartlett, X. Huang and C. Majidi, *Nature Materials*, 2018, DOI: 10.1038/s41563-018-0084-7.
- 20 Y. Osada, H. Okuzaki and H. Hori, *Nature*, 1992, **355**, 242-244.
- 21 E. W. H. Jager, E. Smela and O. Inganas, *Science*, 2000, **290**, 1540-1545.
- 22 S. Li, D. M. Vogt, D. Rus and R. J. Wood, *Proc. Natl. Acad. Sci. U.S.A.*, 2017, **114**, 13132-13137.
- 23 F. Ilievski, A. D. Mazzeo, R. F. Shepherd, X. Chen and G. M. Whitesides, *Angew. Chem., Int. Ed.*, 2011, **50**, 1890-1895.
- 24 R. V. Martinez, J. L. Branch, C. R. Fish, L. Jin, R. F. Shepherd, R. M. D. Nunes, Z. Suo and G. M. Whitesides, *Adv Mater*, 2013, **25**, 205-212.
- 25 E. Smela, *Adv Mater*, 2003, **15**, 481-494.
- 26 Y. Yu and T. Ikeda, *Angew. Chem., Int. Ed.*, 2006, **45**, 5416-5418.
- 27 R. Fuhrer, E. K. Athanassiou, N. A. Luechinger and W. J. Stark, *Small*, 2009, **5**, 383-388.

- 28 S. A. Morin, S. W. Kwok, J. Lessing, J. Ting, R. F. Shepherd, A. A. Stokes and G. M. Whitesides, *Adv. Funct. Mater.*, 2014, **24**, 5541-5549.
- 29 B. Jin, H. Song, R. Jiang, J. Song, Q. Zhao and T. Xie, *Sci. Adv.*, 2018, **4**.
- 30 Q. M. Zhang and M. J. Serpe, *ChemPhysChem*, 2017, **18**, 1451-1465.
- 31 L. Klintberg, M. Karlsson, L. Stenmark, J. A. Schweitz and G. Thornell, *Sens Actuators A Phys*, 2002, **96**, 189-195.
- 32 E. T. Carlen and C. H. Mastrangelo, *J Microelectromech Syst*, 2002, **11**, 165-174.
- 33 R. Pal, M. Yang, B. N. Johnson, D. T. Burke and M. A. Burns, *Anal. Chem.*, 2004, **76**, 3740-3748.
- 34 M. Lehto, R. Bodén, U. Simu, K. Hjort, G. Thornell and J. Å. Schweitz, *J Microelectromech Syst*, 2008, **17**, 1172-1177.
- 35 H. J. Sant, T. Ho and B. K. Gale, *J Microelectromech Syst*, 2010, **20**.
- 36 S. Ogden, L. Klintberg, G. Thornell, K. Hjort and R. Bodén, *Microfluid. Nanofluid.*, 2014, **17**, 53-71.
- 37 Q. Zhao, J. W. C. Dunlop, X. Qiu, F. Huang, Z. Zhang, J. Heyda, J. Dzubiella, M. Antonietti and J. Yuan, *Nat. Commun.*, 2014, **5**.
- 38 M. Ma, L. Guo, D. G. Anderson and R. Langer, *Science*, 2013, **339**, 186-189.
- 39 A. Miriyev, K. Stack and H. Lipson, *Nat. Commun.*, 2017, **8**, 596.
- 40 Y. Liu, J. J. S. Norton, R. Qazi, Z. Zou, K. R. Ammann, H. Liu, L. Yan, P. L. Tran, K. I. Jang, J. W. Lee, D. Zhang, K. A. Kilian, S. H. Jung, T. Bretl, J. Xiao, M. J. Slepian, Y. Huang, J. W. Jeong and J. A. Rogers, *Sci. Adv.*, 2016, **2**.
- 41 R. F. Shepherd, F. Ilievski, W. Choi, S. A. Morin, A. A. Stokes, A. D. Mazzeo, X. Chen, M. Wang and G. M. Whitesides, *Proc. Natl. Acad. Sci. U.S.A.*, 2011, **108**, 20400-20403.
- 42 S. An, Y. I. Kim, M. W. Lee, A. L. Yarin and S. S. Yoon, *Langmuir*, 2017, **33**, 10663-10672.
- 43 L. M. Hansen, D. J. Smith, D. H. Reneker and W. Kataphinan, *J. Appl. Polym. Sci.*, 2005, **95**, 427-434.
- 44 J. T. McCann, M. Marquez and Y. Xia, *J. Am. Chem. Soc.*, 2006, **128**, 1436-1437.
- 45 A. H. Hekmati, N. Khenoussi, H. Nouali, J. Patarin and J. Y. Drean, *Text. Res. J.*, 2014, **84**, 2045-2055.
- 46 S. Jiang, G. Duan, U. Kuhn, M. Mörl, V. Altstädt, A. L. Yarin and A. Greiner, *Angew. Chem., Int. Ed.*, 2017, **56**, 3285-3288.
- 47 S. A. D. J. Kang, and A. L. Yarin, *Nanoscale*, 2018, **10**, 16591-16600.
- 48 A. Miriyev, K. Stack and H. Lipson, *Nature Communications*, 2017, **8**.
- 49 S. M. Jordan and W. J. Koros, *J Polym Sci Part B*, 1990, **28**, 795-809.

TOC



We demonstrate novel thermo-responsive nano-textured bio-mimetic programmable soft actuators based on liquid-vapor phase change. The combination of a soft matrix (silicone-based elastomer) and polyacrylonitrile nanofiber (PAN NF) mat provide a confined structure, which entraps the ethanol and vapor. At the boiling temperature of ethanol (78 °C) vapor expansion causes bending of the encasing flexible matrix. The thermo-responsive actuators can generate strains which determines significant deformation of such actuators.